Available online at www.sciencedirect.com
ScienceDirect
Icarus 188 (2007) 356–366
ICARUS
www.elsevier.com/locate/icarus

# Enceladus: The likely dominant nitrogen source in Saturn's magnetosphere

H.T. Smith [d,*], R.E. Johnson [a], E.C. Sittler [b], M. Shappirio [b], D. Reisenfeld [c], O.J. Tucker [a], M. Burger [b], F.J. Crary [d], D.J. McComas [d], D.T. Young [d]

[a] *Engineering Physics, University of Virginia, Thornton Hall, Charlottesville, VA 22904, USA*
[b] *NASA/Goddard Space Flight Center, 8800 Greenbelt Road, Greenbelt, MD 20771, USA*
[c] *Department of Physics and Astronomy, University of Montana, 32 Campus Drive, Missoula, MT 59812, USA*
[d] *Division of Space Science and Engineering, Southwest Research Institute, 9503 W Commerce, San Antonio, TX 78227-1301, USA*

Received 3 October 2006; revised 29 November 2006

Available online 3 January 2007

**Abstract**

The spatial distribution of $N^+$ in Saturn's magnetosphere obtained from Cassini Plasma Spectrometer (CAPS) data can be used to determine the spatial distribution and relative importance of the nitrogen sources for Saturn's magnetosphere. We first summarize CAPS data from 15 orbits showing the spatial and energy distribution of the nitrogen component of the plasma. This analysis re-enforces our earlier discovery [Smith, H.T., Shappirio, M., Sittler, E.C., Reisenfeld, D., Johnson, R.E., Baragiola, R.A., Crary, F.J., McComas, D.J., Young, D.T., 2005. Geophys. Res. Lett. 32 (14). L14S03] that Enceladus is likely the dominant nitrogen source for Saturn's inner magnetosphere. We also find a sharp enhancement in the nitrogen ion to water ion ratio near the orbit of Enceladus which, we show, is consistent with the presence of a narrow Enceladus torus as described in [Johnson, R.E., Liu, M., Sittler Jr., E.C., 2005. Geophys. Res. Lett. 32. L24201]. The CAPS data and the model described below indicate that $N^+$ ions are a significant fraction of the plasma in this narrow torus. We then simulated the combined Enceladus and Titan nitrogen sources using the CAPS data as a constraint. This simulation is an extension of the model we employed earlier to describe the neutral tori produced by the loss of nitrogen from Titan [Smith, H.T., Johnson, R.E., Shematovich, V.I., 2004. Geophys. Res. Lett. 31 (16). L16804]. We show that Enceladus is the principal nitrogen source in the inner magnetosphere but Titan might account for a fraction of the observed nitrogen ions at the largest distances discussed. We also show that the CAPS data is consistent with Enceladus being a molecular nitrogen source with a nitrogen to water ratio roughly consistent with INMS [Waite, J.H., and 13 colleagues, 2006. Science 311 (5766), 1419–1422], but out-gassing of other nitrogen-containing species, such as ammonia, cannot be ruled out.


*Keywords:* Saturn, magnetosphere; Satellites; Enceladus; Titan

## 1. Introduction

In an earlier paper we showed for the first time that Enceladus could be a source of nitrogen ions in Saturn's inner magnetosphere (Smith et al., 2005). It was subsequently confirmed that Enceladus was indeed a source of neutral nitrogen (Waite et al., 2006). In this paper we extend our earlier analysis using Cassini Plasma Spectrometer (CAPS) data collected during multiple orbits in order to describe the spatial distribution of the $N^+$ in Saturn's magnetosphere. The goal is to determine the nature and relative importance of the Enceladus and Titan nitrogen sources in Saturn's magnetosphere. We first present our analysis of CAPS data from 15 orbits and examine the spatial and energy distribution of the nitrogen ions. Next, we employ a simulation used to describe the neutral tori produced by the loss of nitrogen from Titan (Smith et al., 2004) in order to describe both the Enceladus and Titan sources of nitrogen using the CAPS data as a constraint.

The presence of nitrogen ions in Saturn's magnetosphere can in principal be used to identify parent nitrogen species and sources in the saturnian system. Prior to 2004, much of our data about Saturn was derived from terrestrial and Hubble Space Telescope observations since only three space missions had visited the planet in the form of brief fly-bys (Pioneer 11 and Voyagers 1 and 2) through Saturn's magnetosphere. Of particu-

* Corresponding author.
*E-mail address:* hts4f@virginia.edu (H.T. Smith).

0019-1035/$ – see front matter 
doi:10.1016/j.icarus.2006.12.007

lar interest to this work, Voyagers 1 and 2 detected thermal and energetic plasmas consisting of groups of light and heavier ions (Richardson and Sittler, 1990). While the light ions were identified as protons, Voyager lacked the mass resolution to determine whether the heavier ions were oxygen or nitrogen, limiting our ability to locate nitrogen sources in the saturnian system. Because Titan's nitrogen-rich atmosphere was proposed as a significant source for Saturn's magnetosphere (Barbosa, 1987; Ip, 1997), we simulated the spatial distribution of the nitrogen ion source rate due to loss of atmosphere from Titan (Smith et al., 2004) in anticipation of Cassini's arrival at Saturn. In addition to Titan, primordial nitrogen species trapped (Stevenson, 1982; Squyres et al., 1983) or implanted (Delitsky and Lane, 2002; Sittler et al., 2005) in the icy satellite surfaces were also suggested as potential sources of nitrogen ions for Saturn's magnetosphere.

The arrival of the Cassini spacecraft on July 1, 2004 is rapidly increasing our understanding of Saturn's magnetosphere. In addition to the Huygens probe, the spacecraft carries 12 instruments and has only partially completed a nominal 4-year mission. We derive the results presented here from one of these 12 instruments, the Cassini Plasma Spectrometer (CAPS) (Young et al., 2004). In particular, we use the Ion Mass Spectrometer (IMS) portion of the CAPS to detect ions with energies between 1 eV to 50 keV and a mass per charge ratio ($M/Q$) between 1 and 100 amu/e. The energy resolution ($\Delta E/E$) is 0.17 while the mass resolution ($M/\Delta M$) is ~60 amu/e (Young et al., 2004). The IMS collects ions, selected for a specific mass/charge range and determines a particle's time of flight through the instrument. This time of flight measurement, along with the energy/charge information is then used to determine the original ion's mass.

Prior to the discovery of active "jets" emanating from Enceladus' south polar region (Hansen et al., 2006; Porco et al., 2006), we showed that the nitrogen ions in Saturn's magnetosphere did not appear to be associated with a Titan source but rather appeared to have a source near Enceladus' orbit (Smith et al., 2005). This unexpected discovery provided motivation to use additional Cassini orbits to better understand the spatial distribution and sources of nitrogen ions. The subsequent detection of active, nitrogen containing "jets" emanating from the Enceladus' south polar region (Waite et al., 2006) confirmed our analysis that Enceladus was indeed a source of nitrogen for Saturn's magnetosphere. Since ammonia hydrate has a lower melting temperature than water, ammonia had been suggested as possible volatile species (Squyres et al., 1983). However, molecular nitrogen was apparently detected in the Enceladus plumes at ~4% of the total plume composition level (Waite et al., 2006). While small amounts of ammonia could not be ruled out (e.g., Bouhram et al., 2005; Matson et al., 2006) no positive detection was made. Unfortunately, the predicted magnetospheric neutral nitrogen densities outside a few Enceladus radii are below Cassini neutral detection limits. Therefore, the spatial distribution of nitrogen ions must be used to infer the fate and distribution of the nitrogen in Saturn's magnetosphere. In this paper, we first seek to characterize and identify the nitrogen ion sources and examine whether $N_2$ could be the molecular parent of the detected $N^+$ or is another parent species required.

## 2. CAPS data analysis

Here we describe the energy and spatial distribution of $N^+$ using data collected by CAPS in order to locate nitrogen sources. We expand on our initial detection (Smith et al., 2005) by examining CAPS data collected for the presence of nitrogen ions during 15 Cassini orbits (SOI, Revs A, B, 3, 4, 5, 6, 7, 8, 11, 12, 13, 14, 16, and 17) beginning with the initial orbit (SOI—July 1, 2004) until Rev 17 (October 29, 2005). In order to detect $N^+$ signatures in the CAPS data, we were required to account for background noise, fixed pattern instrument interference and the high energy radiation effects when Cassini is ~ <4.5 Rs from Saturn (Smith, 2006). For this purpose we used the ion mass spectrometer sensor that has high mass resolution, but unfortunately less sensitivity than the straight through detections used to describe the distribution of water ions in Saturn's magnetosphere (Young et al., 2005; Sittler et al., 2006b). It is also important to note that while the nitrogen ions detected are predominately $N^+$, it is possible that a small portion of these ion counts could be $NH_x^+$ with $x = 1$, 2, or 3. We are developing the ability to clearly resolve these species, but for the purposes of this paper, we use $N^+$ to refer to the peak in the spectra that contains atomic nitrogen ions as well as possible small amounts of $NH_x^+$ counts.

Fig. 1 shows the spatial locations of all our $N^+$ detections as a function of radial distance from Saturn, $R$, and distance from the satellite orbit plane, $Z$. We detect $N^+$ furthest from Saturn (~13.5 Saturn radii or "Rs") in the equatorial plane with the maximum radial distance for detection progressively decreasing as the vertical location (above and below the plane) is increased. Assuming the detection limit is due to instrument sensitivity, the pattern in Fig. 1 is suggestive of a spatial distribution similar to that of the OH cloud detected

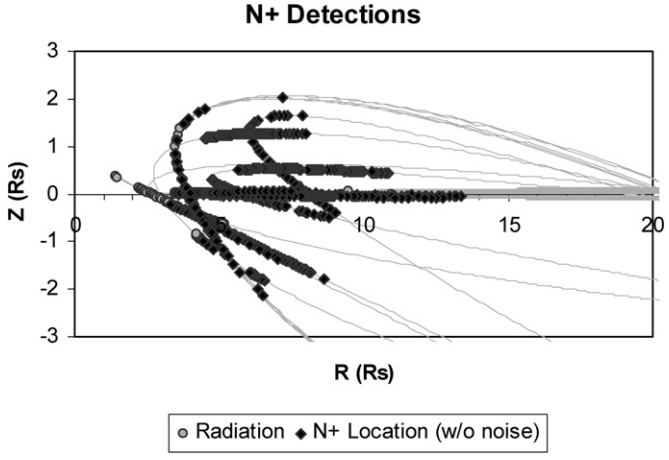


Fig. 1. $N^+$ detection locations. Spatial distribution of all CAPS nitrogen ion detections (black diamonds) as a function of radial distance from Saturn and $Z$-axis location relative to the equatorial plane. Black lines indicate all orbital trajectories and the gray circles show locations with probable $N^+$ but penetrating radiation prevented a positive detection.

using the Hubble Space Telescope (Shemansky et al., 1993; Jurac et al., 2002).

For many of the orbits we examined, CAPS did not actuate and/or the spacecraft was not optimally pointed. As the ion fluxes are not isotropic, a complete sampling of ions was not obtained for such orbits. Therefore absolute ion densities have not been calculated. However, we can provide a measure of relative spatial distributions of $N^+$ for any particular pass for which the CAPS sampling conditions are roughly constant. For such passes the relative amounts of $N^+$ as a function of distance from Saturn can be derived. Because CAPS measures the flux of ions, faster ions give higher relative count rates than slower ions. To account for this using a standard method, the ion flux is converted into a partial phase space density (PSD) ($s^3/m^6$) (Appendix A). The resulting spatial distributions allow us to examine relative increases or decreases in the amounts of $N^+$ as the spacecraft moves through Saturn's magnetosphere during a particular pass. The PSD measurements are integrated over the angles and energies observed during a particular collection period for which all possible energies are sampled (referred to as a "B-cycle"). This yields a single value for each observation rather than density as function of energy. This result, also extracted from Voyager data, is referred to as a reduced distribution function.

Fig. 2 shows example results for the Cassini Rev 4 (March 8, 2005) pass through Saturn's magnetosphere when the spacecraft remained very close to the equatorial plane. The spatial PSD distribution has a maximum chi-square value of 24.7. As with all of our detections, these data show a consistent clearly defined increase in the amount of $N^+$ as the spacecraft moves closer to Saturn with positive detections as far away as ~13.5 Rs.

Fig. 3 shows a compilation of all our CAPS $N^+$ detections divided into three orbit inclination groups relative to the equatorial plane. While all of these detections follow the same basic trend of increasing amounts of nitrogen ions closer to Saturn, they also help illustrate that the closer the inclination to the equatorial plane, the further from Saturn radially that we detect nitrogen ions.

As shown above, the nitrogen ion distribution is a function of distance above/below the equatorial plane as well as the radial distance from Saturn. In the vicinity of ~4–5 Rs, $N^+$ is detected as much as ± ~2 Rs from this plane in the $Z$ direction as seen in Fig. 1. Because of the differences in pointing and actuation in this paper we do not make assumption about the plasma sheet scale height vs $R$. Rather, we have selected all of the $N^+$ detections close to Saturn's orbital plane (±0.25 Rs). We further filtered this data for those orbits during which the instrument is oriented to favorably view the plasma flow and present this phase space density compilation in Fig. 4. As with the Rev 4 orbit in Fig. 2, this figure confirms our earlier discovery (Smith et al., 2005) that the amount of nitrogen in the saturnian equatorial plasma steadily increases with decreasing distance from Saturn to about ~4 Rs (near Enceladus' orbit) where the background becomes a problem.

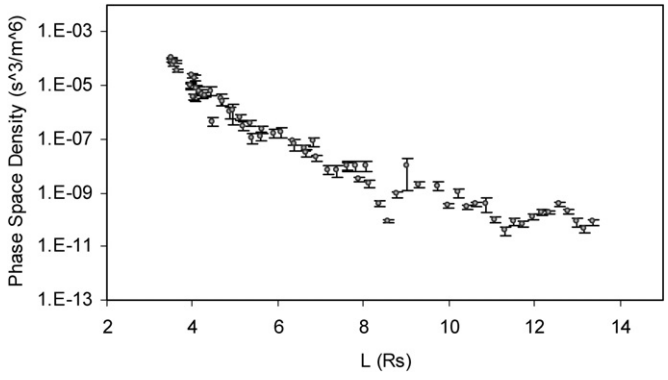


Fig. 2. $N^+$ phase space density for Rev 4. Integrated PSD ($s^3/m^6$) for each nitrogen ion observation as a function of L-shell distance from Saturn for Cassini's 6th (Rev 4) periapsis with 1-sigma error bars.

The $N^+$ spatial distribution compared to that for the water-group ions also provides useful information. Water-group ions dominate the heavy ion population (Young et al., 2005) and appear to be generated by Enceladus (Sittler et al., 2006b). Therefore, the ratio of nitrogen ion PSD to water-group ion PSD (we use $W^+$ to denote the water-group ions; $H_3O^+$, $H_2O^+$, $OH^+$, $O^+$) shows how the relative abundance of $N^+$ compares to the dominant heavier ions vs distance from Saturn. A constant $N^+/W^+$ ratio would suggest similar sources and transport processes for $N^+$ and $W^+$. Conversely, variations in this ratio with distance from Saturn point to specific nitrogen sources or differences in the plasma interactions and transport in Saturn's magnetosphere. Fig. 5 shows the relative $N^+/W^+$ for all data presented in Fig. 4. Notice that, even allowing for the considerable scatter in the data, the ratio is nearly constant but decreases slowly with increasing distance beyond ~4 Rs from Saturn. The insert in Fig. 4 gives the same data for Rev 4. This data set is associated with an orbit in which there is consistent pointing of the CAPS instrument and the spacecraft orbit is close to the equatorial plane throughout the region of interest. It is seen that there is a clear peak in the ratio near the orbit of Enceladus and then a nearly constant ratio at larger $R$.

It is important to note that the CAPS exhibits species-dependent detection efficiencies, so that the absolute ratio values may change as these efficiencies are refined by the instrument team. However, the basic trend seen in the ratio should remain the same. Therefore, we conclude that either the water source rate may be more extended than the nitrogen sources, which would be the case if the E-ring grains, which are likely depleted in nitrogen, contributed away from Enceladus or the plasma interactions and transport processes differ so that the nitrogen ion density decreases slightly faster than the water ion density with increasing $R$.

The average energy of $N^+$ ions is also suggestive of the source location. Fig. 6 illustrates spatial distribution of average energies for the $N^+$ detections as a function of distance from Saturn. Additionally, a dotted line represents the co-rotational energy with associated Keplerian orbital energy removed because fresh pick-up ions formed locally would have an average energy roughly proportional to $(v_{co} - v_o)^2$, where $v_{co}$ is the co-rotational speed and $v_o$ is the Keplerian orbit speed. In addition, Young et al. (2005) showed the plasma electrons are likely heated by the ions in this region and, therefore, the average

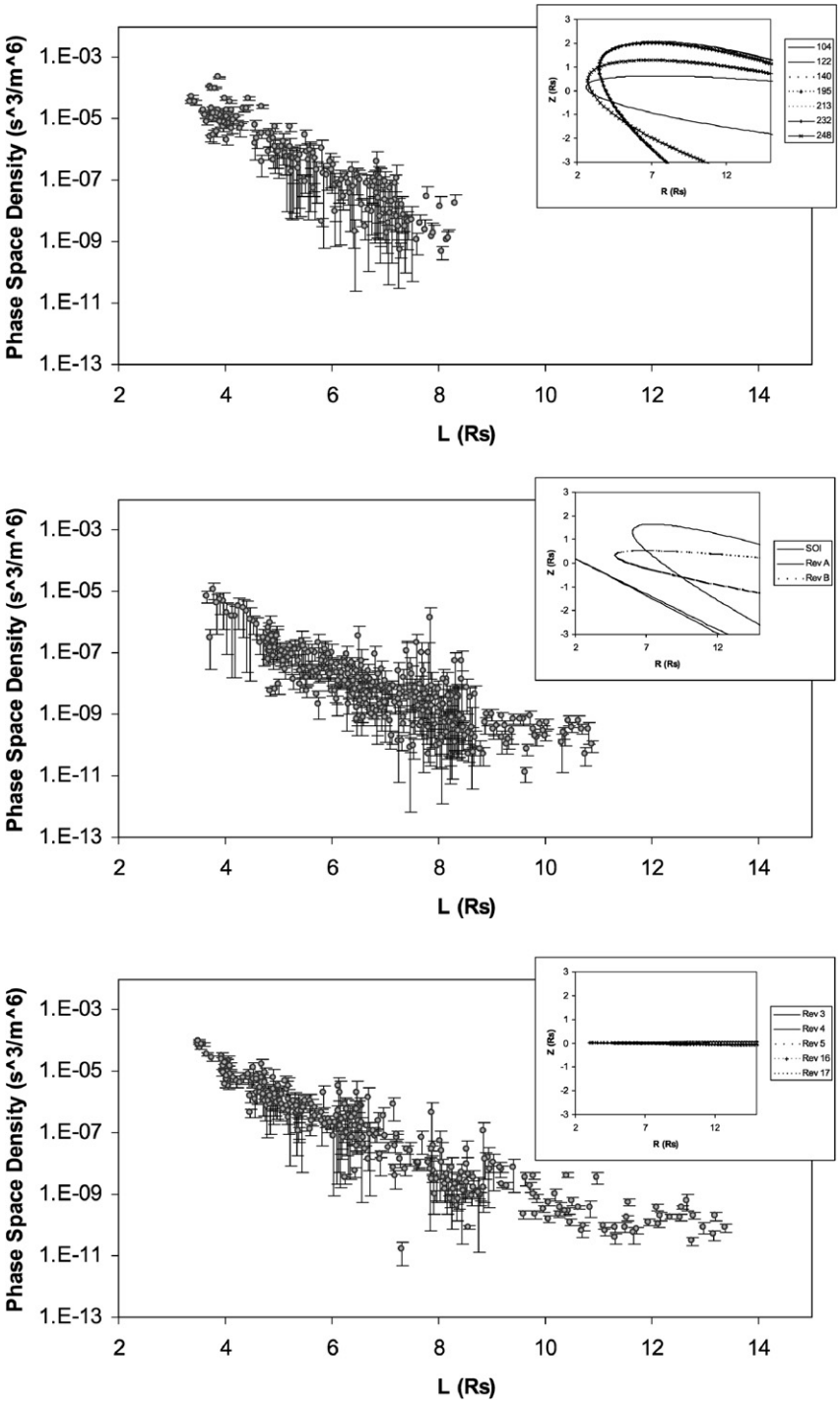


Fig. 3. $N^+$ phase space density for all examined orbits. Integrated PSD ($s^3/m^6$) for each nitrogen ion observation as a function of L-shell distance from Saturn for Revs 6, 7, 8, 11, 12, 13, 14 (top panel—highest inclinations); SOI, Revs A, B (middle panel—lower inclinations); Revs 3, 4, 5, 16, 17 (bottom panel—lowest inclinations) with 1-sigma error bars. Insets plot the associated orbital trajectories as a function of radial distance from Saturn ($R$) and $Z$-axis location relative to the equatorial plane.

ion energies are below the co-rotation energy. If the detected $N^+$ ions were being generated much further away from Saturn (at Titan's orbit, for example) and then diffused inward by plasma transport processes, they would have much higher energies ($\gg$10 keV; e.g., Sittler et al., 2006a). Therefore, the detected ions were principally produced at distances much closer to Saturn than Titan's orbit.

Since the nitrogen PSD values are largest and the $N^+$ to $W^+$ ratio is also slightly higher near the orbit of Enceladus, we focused on the July 14, 2005 (DOY 195) close fly-by of this moon. This orbit was selected because Cassini passed within ~170 km of Enceladus' surface. The left panel of Fig. 7 shows Cassini's orbital trajectory (gray line) in the $X$–$Y$ plane with Saturn at the center and the $X$-axis pointed toward the Sun.

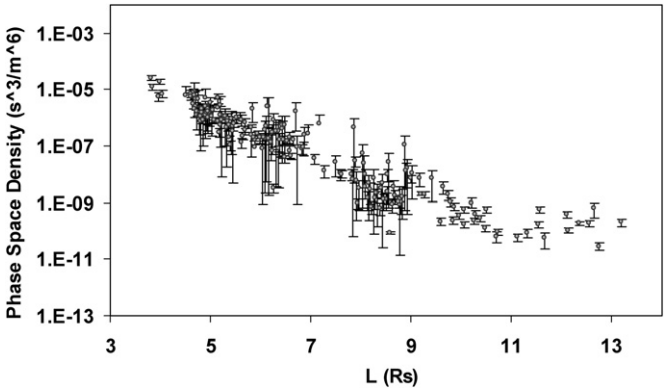


Fig. 4. Nitrogen ion PSD ($Z < |0.25$ Rs|). Reduced distribution function PSD ($s^3/m^6$) for nitrogen ion observations (within ±0.25 Saturn radii of the orbital plane) as a function of L-shell distance from Saturn for all analyzed Cassini's orbits with 1-sigma error bars. Enceladus orbital shell noted.

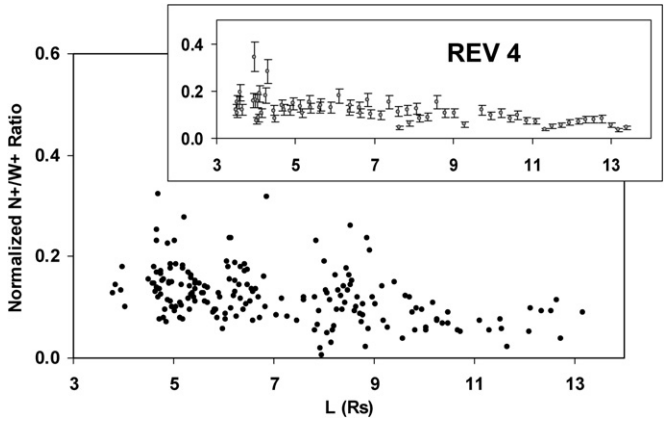


Fig. 5. Nitrogen to water-group ion ratio (all detections). Ratio of $N^+$ phase space density to water-group ion ($W^+$) phase space density for each B-cycle observation as a function of L-shell (black dots) for all analyzed orbits. Inset: the same data for only Rev 4 that indicates an $N^+$ enhancement at Enceladus' orbit (error bars are the greater of the 1-sigma and $W^+$ mass uncertainty errors).

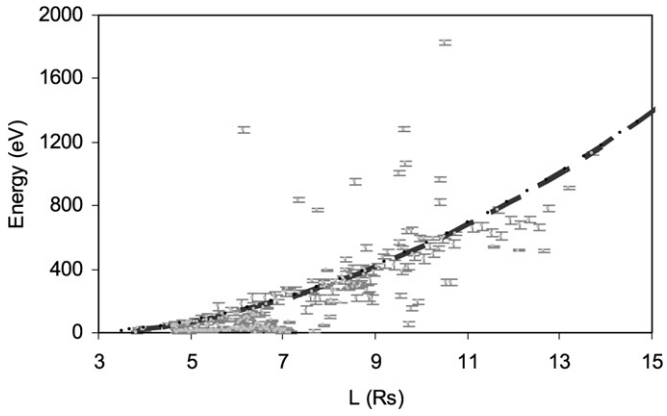


Fig. 6. $N^+$ average energy (all detections). Average energy (eV) for each B-cycle observation as a function of L-shell for all analyzed orbits (black dots). The dotted line approximates $N^+$ pick-up energy based on co-rotational velocity minus the orbital velocity.

Additionally, Enceladus' orbit is represented by the black circle. The right panel of this figure is the relative $N^+/W^+$ ratio displayed as a function of time relative to closest approach to Enceladus. The relative amount of nitrogen appears to be enhanced around closest approach indicated by the left most vertical dotted line which coincides to the location indicated in the left panel. An enhancement is again seen near the second orbit crossing. This is the point when the spacecraft crosses Enceladus' orbit (indicated in the left panel), but it is now >50,000 km ahead of the moon. Thus we see a $N^+$ enhancement very close to Enceladus as well as further away along the moon's orbital trajectory. This enhancement, consistent with the Rev 4 data in Fig. 5, is a marker for the presence of the narrow, dense Enceladus torus described in Johnson et al. (2006). The small shift in the maximum in the ratio to a radius slightly larger than that of Enceladus is consistent with the neutral cloud model.

That the ratio in the narrow Enceladus torus is enhanced over the ratio of the neutral source rates is readily understood. Since the plasma is dominated by $W^+$ and charge exchange is the dominant neutral loss and ionization process, nitrogen is ionized primarily by charge exchange with $W^+$ ions, but, although the charge exchange process ($W^+ + W \rightarrow W + W^+$) produces mass loading (Burger et al., 2006), it does not produce additional water product ions. Additional $W^+$ are only produced by electron and photon impact ionization, so that the ratio of nitrogen ions ($N^+$ and $N_2^+$) to $W^+$ is enhanced over the ratio of the sources as described in Appendix B and discussed below. Therefore, the CAPS data and the model below indicate that nitrogen ions are a significant fraction of the plasma in the narrow Enceladus torus. Further, as the peak is seen downstream from Enceladus, this torus is likely toroidal as indicated by the models (e.g., Johnson et al., 2006; Burger et al., 2006).

## 3. Nitrogen torus simulations and Cassini observations

Based on the above observations, the nitrogen ion densities increase inward toward Enceladus rather than outward toward Titan. This confirms the result reported in our earlier paper (Smith et al., 2005) in which we first reported nitrogen ions originating from Enceladus. Although the Cassini Ion Neutral Mass Spectrometer (INMS) apparently detected molecules with a mass of 28 amu (Waite et al., 2006) as Cassini flew through the Enceladus 'jets,' our present analysis of CAPS data does not clearly indicate the presence of $N_2^+$. Therefore, we have modeled nitrogen sources from Enceladus and Titan in order to examine the possibility that the $N^+$ we detected could have indeed originated from any possible $N_2$ detected by INMS or if another nitrogen species was required by the CAPS observations.

Since the dominant nitrogen ion source appears to be near Enceladus, we updated our earlier simulations for loss of nitrogen from Titan (Smith et al., 2004) by including an Enceladus source (Smith, 2006). Whereas both N and $N_2$ were ejected from Titan's upper atmosphere (Michael et al., 2005; Shematovich et al., 2003), we assumed that the Enceladus source is only molecular nitrogen. Waite et al. (2006) found that water is the main component of the Enceladus jets at ∼91% while $N_2$ constituted ∼4% of the total plume composition us-

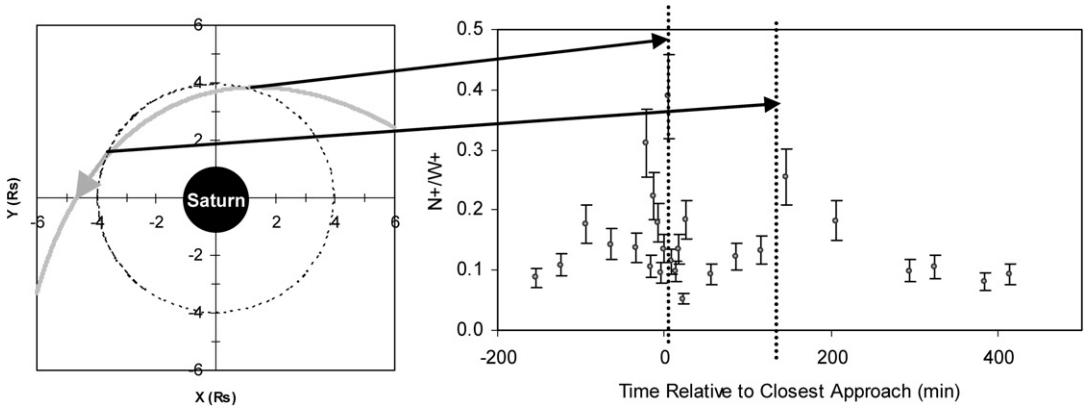


Fig. 7. Nitrogen to water-group ion ratio ($Z < |0.25$ Rs$|$). Right panel: ratio of $N^+$ phase space density to water-group ion ($W^+$) phase space density as a function of time relative to closest approach (minutes) during the 14 July 2005 Enceladus encounter (error bars are the greater of the 1-sigma and $W^+$ mass uncertainty errors). Left panel: geometric plot (in equatorial plane) of the encounter: Cassini trajectory (gray line); Enceladus orbit (black dotted line). Dotted black line relates $N^+/W^+$ data to encounter locations.

ing the INMS instrument or 8% N atoms per water molecule. While the velocity of the escaping gas is not known, the jets are currently assumed to eject particles at velocities associated with a source temperature of ~145–180 K (Hansen et al., 2006; Spencer et al., 2006) from the south pole tiger stripes. Therefore, as with our earlier work on the Enceladus water torus (Johnson et al., 2006) we assumed that the $N_2$ is ejected with a Maxwellian flux distribution represented by

$$f(E) = \frac{E e^{(-E/(kT))}}{(kT)^2}, \tag{1}$$

where $E$ is the particle's energy and $T = 180$ K. We also assume that this nitrogen is only ejected from the south polar tiger stripes with a cosine angular distribution. This source rate is equivalent to a thermal distribution with $T = 180$ K, superimposed on a flow speed of ~360 m/s (Johnson et al., 2006). Based on an assumed flow speed, Hansen et al. (2006) used their measured column density to estimate a source rate of ~0.5–1 $\times 10^{28}$ particles/s. Here we use the water source rate ($10^{28}$ $H_2O$/s) used in Johnson et al. (2006) to populate both the OH cloud and the Enceladus torus. Assuming a 4% concentration, we use a nitrogen source rate ~$2 \times 10^{26}$ $N_2$/s.

Based on CAPS data, Sittler et al. (2006b) gave new plasma parameter values for radial distances <10 Rs from Saturn. Therefore, we updated the model plasma parameters in Smith et al. (2004) for this region and scaled the earlier densities for distances >10 $R$ in order to calculate revised neutral particle lifetimes. Fig. 8 shows the N and $N_2$ lifetimes along the equatorial plane using appropriate cross sections (Basu et al., 1987; Cosby, 1993; Flesch and Ng, 1990; Freund et al., 1990; Phelps, 1991; Rees, 1989; Stier and Barnett, 1956) as described in Smith (2006). Since Sittler et al. (2006b) provided plasma parameters as a function of elevation and radial distance; we also calculated lifetimes vs distance above and below the equatorial plane.

Because CAPS detects nitrogen ions and not neutrals, we also computed ion lifetimes in order to compare model $N^+$ to $N_2^+$ densities to the detected ion PSD. We used cross sections for the nitrogen ion charge exchange with water (Dressler et al., 1993, 1995) along with the neutral cloud densities from Jurac and Richardson (2005) to calculate lifetimes for nitrogen ion charge exchange with neutral water products. Additionally, we upgraded those neutral cloud densities with our model neutral water densities close to Enceladus to include the sharp density increase near the orbit of this moon (Johnson et al., 2006). We also used the Sittler et al. (2006b) electron densities and temperatures to compute $N_2^+$ recombination lifetimes (Sheehan and St.-Maurice, 2004). Because these ions are distributed non-uniformly, they can diffuse radially outward or inward from the source region resulting in the loss of ions locally. Sittler et al. (2006a) treated this as a loss process using an average diffusion lifetime given by

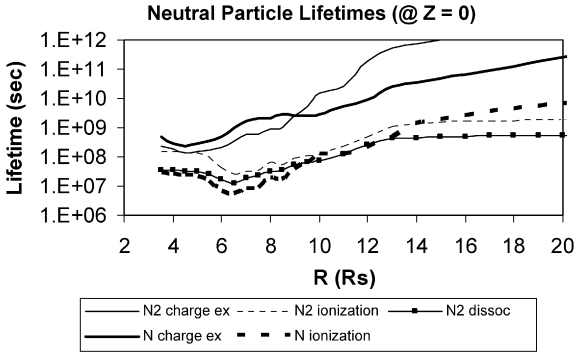


Fig. 8. Neutral lifetimes. Plot of neutral nitrogen lifetimes (seconds) vs radial distance from Saturn (Rs) in the equatorial plane ($Z = 0$) derived using new Sittler et al. (2006b) plasma parameters: $N_2$ charge exchange (solid line), $N_2$ electron impact and photoionization (dashed line), $N_2$ dissociation (solid line with squares), N charge exchange (thick solid line), and N ionization (thick dashed line).

$$\tau = (4.32 \times 10^5 \text{ s})\left(\frac{6.3}{L}\right)^3, \tag{2}$$

where $1/\tau$ is the loss rate and $L$ is the dipole-L shell. Although one should ultimately solve the ion diffusion equation, this lifetime is suggestive of the relative importance of diffusion. These lifetimes, discussed further in Smith (2006), are in Fig. 9. It is seen that beyond about 5 Rs diffusion dominates the nitrogen

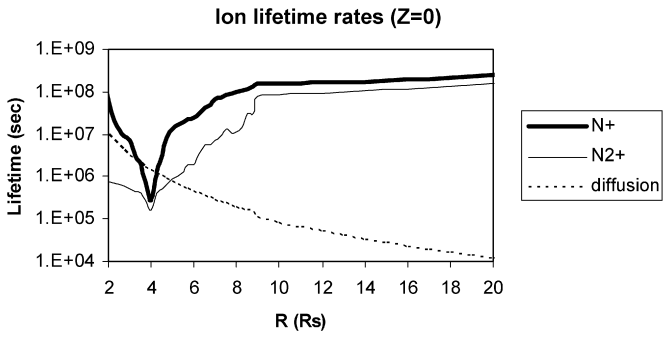


Fig. 9. Updated nitrogen ion lifetimes. Plot of $N^+$ and $N_2^+$ lifetimes (seconds) vs radial distance from Saturn (Rs) in the equatorial plane ($Z = 0$) based on Sittler et al. (2006b) plasma parameters, Jurac and Richardson (2005) water cloud parameters and near-Enceladus cloud modeling: $N^+$ (thick solid line), $N_2^+$ (solid line), and diffusion (dotted line).

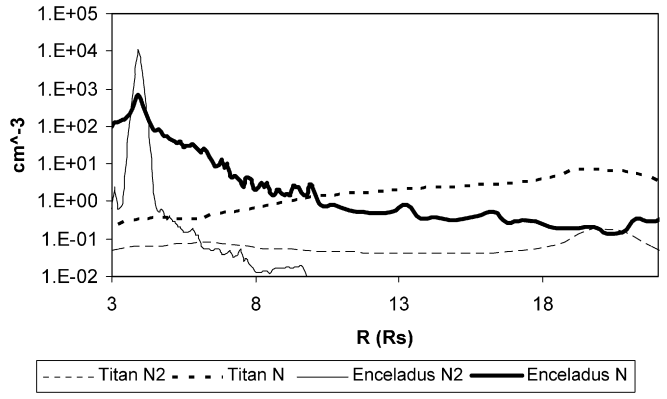


Fig. 10. Model neutral nitrogen densities ($cm^{-3}$) vs radial distance from Saturn (Rs) in the equatorial plane ($Z = 0$). Thin lines represent $N_2$ and thick lines for N, solid lines for the Enceladus source and dashed lines for the Titan source.

ion loss rate. It is also seen that near Enceladus the $N^+$ are lost primarily by charge exchange with water molecules.

Using the new plasma parameters and lifetimes discussed above and our computational model, we recalculated the neutral and ion tori densities and the ion source rates using the $N_2$ source from Enceladus and the Titan N and $N_2$ sources used earlier. To account for neutral particle recycling (Johnson et al., 2005, 2006), we identify the amount of nitrogen that is ionized and subsequently neutralized by charge exchange or, for $N_2^+$, by electron–ion recombination producing two N atoms. Our model returns these neutral particles to the neutral cloud with the appropriate energy modification from the ionization/recombination process. Although our model produces three-dimensional results, we present only the results along the equatorial plane in order to compare to the CAPS $N^+$ data presented above.

The results given in Fig. 10 show the neutral torus densities from each source as a function of radial distance from Saturn. The peak densities are at Titan's orbit (∼20 Rs) and Enceladus' orbit (∼4 Rs). First we note that Titan is still seen to be a direct source of nitrogen for the inner magnetosphere as shown earlier (Smith et al., 2004). However, these results clearly show that Enceladus is the dominant neutral nitrogen source in the inner magnetosphere. Throughout much of the region, the N density

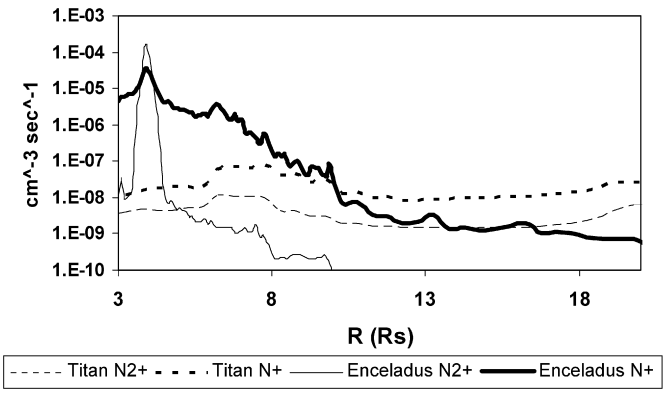


Fig. 11. Model nitrogen ion source rates. Computational model nitrogen ion source rates ($s^{-1}\,cm^{-3}$) vs radial distance from Saturn (Rs) in the equatorial plane ($Z = 0$) using ion lifetimes described. Thin lines represent $N_2^+$, thick lines for $N^+$, solid lines for the Enceladus nitrogen source, and dashed lines for the Titan source.

exceeds the density of $N_2$. Close to Enceladus the molecular nitrogen densities are, not surprisingly, higher than the atomic densities. Although the Enceladus source in this simulation is molecular, N atoms dominate the neutral cloud beyond <1 Rs from Enceladus' orbit because the $N_2$ dissociation rate is much faster than the $N_2$ ionization rate.

Our model also generates nitrogen ion production rates from the neutral nitrogen cloud. Since the CAPS instrument measures ion density and not source rates, we multiplied these rates by the ion lifetimes. Beyond ∼5 Rs, where diffusion dominates, this procedure underestimates the ion densities. The resulting ion source rates as a function of radial distance from Saturn are given in Fig. 11. Using these sources rates along with ion lifetimes discussed, we derived the ion densities as a function of radial distance from Saturn. We find in Fig. 12a, consistent with CAPS data, that the ion densities decrease with distance from the Enceladus torus and $N^+$ completely dominates $N_2^+$ over most of the region in which detections were made. However, these simulations also show that the $N_2^+$ densities are comparable to the $N^+$ densities in the Enceladus narrow torus region. Since the INMS sensitivity was only sufficient to detect $N_2$ within a few hundred kilometers of the source, the only test of these simulations is the CAPS ion data.

The total calculated model $N^+$ densities are compared to the PSD data for Rev 4 in Fig. 12b. It is seen that the $N^+$ density exhibits a trend roughly similar to that seen in the $N^+$ PSD distributions. The trends would in fact be more similar if the Titan source was removed. However, this is a region in which we treated diffusion very crudely, and to obtain the density from the PSD distribution requires integration over the speed distribution. Since the mean speed of the plasma is increasing with increasing $R$ (Fig. 6) the PSD decreases somewhat faster than the actual $N^+$ density. We will conduct more detailed simulations; however, these simulations confirm that Enceladus is the dominant source of $N^+$ out to about 10 Rs. This is the case even in the absence of other possible inner magnetospheric sources. Interestingly, the simulations also suggest that Titan could be a measurable contributor to the $N^+$ densities at the largest radii at which we detected $N^+$.

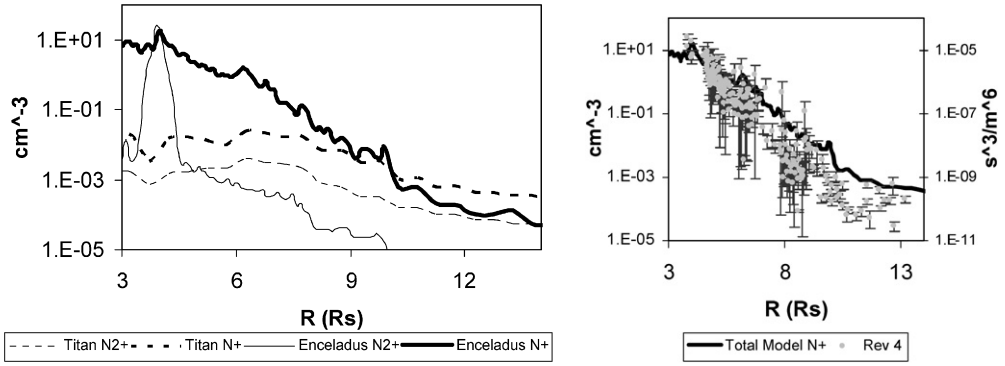


Fig. 12. Model nitrogen ion densities. Computational model nitrogen densities ($cm^{-3}$): (a) vs radial distance from Saturn (Rs) in the equatorial plane ($Z = 0$) using ion lifetimes described. Thin lines represent $N_2^+$, thick lines for $N^+$, solid lines for the Enceladus nitrogen source, and dashed lines for the Titan source. Panel (b) compares the Rev 4 PSD to our total model $N^+$ density.

Although $N_2$ from Enceladus is the dominant nitrogen source in these simulations and $N_2$ dominates the neutral cloud, it is interesting that $N^+$ is the dominant ion over most of the region when dissociation and dissociative recombination processes are included. Therefore, the $N^+$ we detected in Saturn's inner magnetosphere using CAPS does not appear to be inconsistent with an $N_2$ Enceladus source except, possibly, very close to Enceladus' orbit where the simulations show there should be a significant $N_2^+$ density. The calibration data for CAPS show that $N_2^+$ peaks are much broader than the $N^+$ peaks due to break-up of the molecular ions in the foil. Therefore, the CAPS ability to identify $N_2^+$ is lower than that for $N^+$. This situation is exacerbated close to Enceladus where the simulations suggest the $N_2^+$ density is largest but is in a region in which CAPS encounters a very high radiation background. Therefore, $N_2^+$ is much more difficult for CAPS to detect in this region than $N^+$. Such a detection is eventually needed to confirm that $N_2$ is the principal source of nitrogen. This evaluation is in progress.

In order to compare our simulation densities to absolute densities, we use the Sittler et al. (2006b) equatorial ion densities at 4.5 Rs ($\sim$30 $W^+/cm^3$). This is outside of the narrow Enceladus torus (Johnson et al., 2006) and inside of the region in which diffusion dominates as discussed above. Our model $N^+$ ion density in Fig. 11b at 4.5 Rs is $\sim 4/cm^3$ and roughly consistent with the average $N^+/W^+$ ratio in Fig. 5 of $\sim$0.15. Work on obtaining good absolute values of $N^+$ density from CAPS data is in progress.

The lifetimes above can also be used to examine the $N^+/W^+$ ratio in the Enceladus torus. In this region ion loss is dominated by charge exchange and electron–ion recombination. In addition, the neutral lifetimes are long, so the torus is fairly uniform (Johnson et al., 2006) and the average properties can be considered. Therefore, in Appendix B we give simplified chemical rate equations that are applicable in this region including $N_2$, N, W, $N_2^+$, $N^+$, and $W^+$, where W accounts for all the water products (Young et al., 2005). In this chemical model we also assume an $N_2$ Enceladus source and the average lifetimes for W and $W^+$ are taken from Burger et al. (2006). In steady state we write the $N^+/W^+$ ratio measured by CAPS as proportional to the $N_2$/W source rates from INMS. Using the lifetimes discussed we find that for a 4% $N_2$ source, the $N^+/W^+$ ratio in the torus is $\sim$0.42 or a factor of $\sim$4.8 enhancement over the ratio of total nitrogen atoms to water molecules. Although this simple model slightly overestimates the ratio, this value is roughly consistent with the ion ratio measured by CAPS. This again suggests that the data is consistent with an $N_2$ source. Based on the data in Fig. 7, the $N^+/W^+$ ratio decreases rapidly outside of the Enceladus torus becoming closer to the source rate ratio for N/W (0.08). This is consistent with the fact that diffusion does not play a dominant role near Enceladus and the region outside the Enceladus torus is populated by the charge exchange redistribution described earlier for the dominant water products (Johnson et al., 2005, 2006).

## 4. Summary

In this paper, we used the total CAPS database through Rev 17 to produce good spatial distributions of the nitrogen ions in Saturn's magnetosphere. We give phase space densities and average energies close to the equatorial plane and the ratio of nitrogen density to the dominant water product ion density from $\sim$4 to 13 Rs. The spatial distribution of $N^+$ strongly supports our earlier indication (Smith et al., 2005) that Enceladus is the principal source of nitrogen ions for Saturn's inner magnetosphere. That the observed nitrogen ions are from an inner magnetospheric source is also consistent with their average energies. Using current CAPS species-dependent detection sensitivities, we also detected a larger $N^+/W^+$ ratio ($\sim$0.15–0.4) within the narrow Enceladus torus region discussed in Johnson et al. (2006). This enhancement over the ratio in the neutral source rate (N/W $\sim$ 0.08) suggested by the INMS data (Waite et al., 2006) occurs because the dominant new ion production and loss processes for $N^+$ are charge exchange with the dominant ions and neutrals in the Enceladus torus which are water products.

We then combined the $N^+$ data with the data for dominant plasma species to update our earlier nitrogen tori model (Smith et al., 2005). The simulations included both Enceladus and Titan sources and all of the principal ionization and charge exchange processes but treated diffusion in an overly simpli-

fied way as a local loss process. Using these simulations, we generated ion densities that roughly correlate to the spatial distribution in the $N^+$ count rates presented earlier (Smith et al., 2005) and to the spatial distribution in the $N^+$ phase space density. The calculated densities in the region where plasma diffusion processes are small appear to be close to the rough absolute $N^+$ densities suggested by the CAPS data. Because CAPS only positively detected $N^+$ but not $N_2^+$, a goal of the simulation was to test whether or not the principal parent nitrogen-containing molecule could be $N_2$. The simulations showed that if one assumes $N_2$ is the dominant nitrogen species out-gassed from Enceladus (Waite et al., 2006), then $N^+$ and not $N_2^+$ is the dominant nitrogen ion throughout most of the magnetosphere, except very close to the orbit of Enceladus. Accounting for the detection efficiency in this region, the dominant signal in the full region studied would be $N^+$ in agreement with CAPS data. Therefore, at present there is no need to assume either additional nitrogen sources, such as the icy E-ring grains, nor is there any need to have additional parent molecules such as $NH_3$ (this may change as further data are analyzed). However, the $N_2$ may originate from $NH_3$ below the surface of Enceladus.

The simulation results in Fig. 12a also showed that a Titan generated neutral nitrogen torus might provide a detectable source of nitrogen ions in the region outside of about 10 Rs. However, because we treated diffusion as a local loss process, this region could also be populated though diffusion processes such as flux tube interchange from smaller values of $R$.

While this work showed that Titan might be a non-negligible nitrogen ion source less than ∼13 Rs from Saturn, it also raises questions about the Titan-generated nitrogen torus at larger $R$. This moon's nitrogen-rich atmosphere is clearly a source of nitrogen ions (Smith et al., 2004; Michael et al., 2005); however, we have not detected any such ions further than ∼13 Rs from Saturn. Based on our simulations, we may be reaching a CAPS $N^+$ detection limit ($\sim 10^{-4}/\mathrm{cm}^3$) beyond ∼13 Rs. However, if their lifetimes were sufficient we should have detected nitrogen ions in the vicinity of Titan's orbit. Either our estimated Titan nitrogen source rates are too large or some magnetospheric loss process is preventing these ions from accumulating, which will be the focus of further research. In particular, nitrogen ions in the vicinity of Titan's orbit may be escaping down Saturn's magnetotail before accumulating detectable ion densities. We will also work on better constraining the $N^+$ densities in order to eliminate other satellites or the E-ring grains as sources of nitrogen. As Cassini's orbital inclination increases over the next two years, more data at varied spatial locations will become available allowing us to better define the out-of plane densities.

Finally, based on our simulations, a direct $NH_3$ Enceladus source does not appear to be necessary to generate the $N^+$ densities detected by CAPS. However this issue needs to be examined more closely as the CAPS data is further analyzed since the possible presence of ammonia can have a dramatic impact on internal water melting temperatures (e.g., Matson et al., 2006) and thus would help explain the observed Enceladus jets. Future Enceladus fly-bys should allow us to compare relative nitrogen concentrations measured over a longer period of time to possibly infer Enceladus plume variability. Additionally, a planned extended mission may take the spacecraft within 25 km of the surface of Enceladus and could provide nitrogen composition information closer to the plume. This will require better understanding the role of penetrating radiation in the CAPS data. The results presented here confirm our earlier discovery that Enceladus is the dominant source of the nitrogen plasma in Saturn's inner magnetosphere. Our results also appear to confirm the presence of a narrow Enceladus torus in which the nitrogen ions are a considerable fraction of the plasma although the neutral source rate is a small fraction of the total. Considering the vast quantities of data collected and that Cassini is half way through its nominal mission, we should be able to resolve the issues discussed above.

## Acknowledgments

This work is supported by JPL contract 1243218 for CAPS operations and data analysis, the NASA Planetary Atmospheres and Outer Planets Programs, NASA GSRP, and the Virginia Space Grant Consortium.

## Appendix A

The CAPS measures the flux of ions into the instrument. Therefore, faster ions give higher relative count rates than slower ions. To account for this in the standard way, we converted the flux of ions flowing into the instrument into a partial phase space density (PSD) ($\mathrm{s}^3/\mathrm{m}^6$) as discussed below which includes the ion counts from only the portion of space that CAPS is able to view. PSD provides a result analogous to a true density by weighting ion counts by their speeds. While we cannot produce a total PSD when the instrument is not actuating, our data provide enough information to examine relative increases or decreases in the amounts of $N^+$ as the spacecraft moves through Saturn's magnetosphere during a particular pass. Additionally, the PSD calculations are integrated over the angles and energies observed during a particular instrument collection cycle which yields a single value for each observation rather than density as function of energy. This result, used on Voyager data, is referred to as a reduced distribution function which is a function of positions and velocities $(x, y, z, v_x, v_y, v_z)$ and thus accounts for the energy dependence in the count rate and has the units of $\mathrm{s}^3/\mathrm{m}^3$. Our method is defined using

$$\mathrm{PSD} = \sum_{i=1}^{n} \frac{(Ci \times m_s^2)}{(2 \times \tau \times \varepsilon_s \times G \times q_s^2 \times e^2 \times E_i^2)}, \tag{A.1}$$

where $C$ is ion counts, $s$ is the species, $i$ is the detection energy level (32 energy bins from ∼1 eV to ∼50 keV, $q$ is the ion charge/nucleon (1 for single charged, 2 for double, etc.), $e$ is electron charge (coulombs), $E$ is the particle energy (eV) and the current CAPS values of

$$\begin{aligned}
&\text{IMS time interval:} \quad \tau \sim 64 \times 0.055 \text{ s},\\
&\text{Detector efficiency:} \quad \varepsilon = 0.0094\ (N^+), 0.0064\ (O^+),\\
&\quad 0.0059\ (OH^+), 0.0058\ (H_2O^+), \text{ and } 0.0055\ (H_2O^+),\\
&\text{Geometric factor:} \quad G \sim 1.5 \times 10^{-7}\ \mathrm{m}^2\,\mathrm{sr\,eV/eV}.
\end{aligned} \tag{A.2}$$

The above values are subject to slight modifications as CAPS calibration activities progress.

## Appendix B

In order to estimate the nitrogen ion to water ion ratio in the Enceladus torus, we first assume that $N_2$ is rapidly dissociated by the low energy electrons in this region and then correct this assumption later. We write the rate equations for the neutral nitrogen ($n_N$) and water-group ($n_W$) densities as

$$\frac{d(n_N)}{dt} = -n_N\left[\frac{1}{\tau_{Ni}} + \frac{1}{\tau_{Nct}}\right] + S_N, \tag{B.1}$$

$$\frac{d(n_W)}{dt} = -n_W\left[\frac{1}{\tau_{Wi}} + \frac{1}{\tau_{Wct}}\right] + S_W, \tag{B.2}$$

where $\tau_{Ni}$ and $\tau_{Wi}$ are the lifetimes of N and W due to electron and photon impact ionization, the $\tau_{Nct}$ and $\tau_{Wct}$ are the charge exchange lifetimes, and the $S$'s are the neutral particle source rates. For ions ($n_{N^+}$ and $n_{W^+}$), the rate equations using $\tau_{Nio}$ and $\tau_{Wio}$ as the net ion loss times are

$$\frac{d(n_{N^+})}{dt} = n_N\left[\frac{1}{\tau_{Ni}} + \frac{1}{\tau_{Nct}}\right] - n_{N^+}\left[\frac{1}{\tau_{Nio}}\right], \tag{B.3}$$

$$\frac{d(n_{W^+})}{dt} = n_W\left[\frac{1}{\tau_{Wi}}\right] - n_{W^+}\left[\frac{1}{\tau_{Wio}}\right]. \tag{B.4}$$

We have assumed that the ions are predominantly $W^+$ and, therefore, W charge exchange does not produce a new ion. It is, however, a neutral loss process as the exiting neutrals from charge exchange mostly have sufficient energy to leave the narrow Enceladus torus populating the larger secondary torus seen by the Hubble Space Telescope (Johnson et al., 2006). Therefore, the ion density ratio in steady state is

$$\frac{n_{N^+}}{n_{W^+}} = \left(\frac{S_N}{S_W}\right)\left(\frac{\tau_{Nio}}{\tau_{Wio}}\right)\left[1 + \frac{\tau_{Wi}}{\tau_{Wct}}\right]. \tag{B.5}$$

Using $S_N/S_W \sim 0.087$ (Waite et al., 2006), $\tau_{Nio} \sim 3.1 \times 10^5$ s, $\tau_{Wio} \sim 4 \times 10^5$ s the value for $(\tau_{Wi}/\tau_{Wct})$ of $(1.1 \times 10^8 s)/(1.4 \times 10^7$ s) or ~10, the enhancement over the ratio of the source rates is ~6.7 ($N^+/W^+ \sim 0.6$).

Including the dissociation of molecular nitrogen into the estimate above requires the following rate equation:

$$\frac{d(n_{N_2})}{dt} = -n_{N_2}\left[\frac{1}{\tau_{N_2D}} + \frac{1}{\tau_{N_2i}} + \frac{1}{\tau_{N_2ct}}\right] + S_{N_2} \tag{B.6}$$

with $S_N$ in Eq. (B.1) replaced by

$$S_N = 2n_{N_2}\left[\frac{1}{\tau_{N_2D}}\right]. \tag{B.7}$$

Here $\tau_{N_2D}$ is the dissociation lifetime. Again assuming steady state for the average values in the Enceladus torus gives

$$n_{N_2} = S_{N_2}\left[\frac{1}{\tau_{N_2D}} + \frac{1}{\tau_{N_2i}} + \frac{1}{\tau_{N_2ct}}\right]^{-1} \tag{B.8}$$

and therefore

$$S_N = 2S_{N_2}\left[1 + \tau_{N_2D}\left(\frac{1}{\tau_{N_2i}} + \frac{1}{\tau_{N_2ct}}\right)\right]^{-1}. \tag{B.9}$$

These equations reduce the ratio in Eq. (B.5) by the fraction of $N_2$ ionized before dissociating to N. Therefore, the full ratio is

$$\frac{n_{N^+}}{n_{W^+}} = \left(\frac{2S_{N_2}}{S_W}\right)\left(\frac{\tau_{Nio}}{\tau_{Wio}}\right)\left[1 + \frac{\tau_{Wi}}{\tau_{Wct}}\right] \times \left[1 + \tau_{N_2D}\left(\frac{1}{\tau_{N_2i}} + \frac{1}{\tau_{N_2ct}}\right)\right]^{-1}. \tag{B.10}$$

Using $\tau_{N_2D} \sim 3.4 \times 10^7$ s, $\tau_{N_2i} \sim 1.4 \times 10^8$ s, $\tau_{N_2ct} \sim 1.9 \times 10^8$ s and the above values gives a $N^+/W^+$ ratio which is ~4.8 times ($2S_{N_2}/S_W$) or $N^+/W^+ \sim 0.42$. One can further improve this model by separating the plasma into the fraction that is nitrogen versus the fraction that is $W^+$, since in the Enceladus torus the $N^+$ density is not negligible. In doing this one should also include small fraction of protons in the plasma. More detailed simulations are in progress. However, these estimates indicate that the combination of $N_2^+$ and $N^+$ can be a significant fraction of the plasma in the Enceladus torus.

## References


Barbosa, D.D., 1987. Titan's atomic nitrogen torus: Inferred properties and consequences for the saturnian aurora. Icarus 72, 53–61.

Basu, B., Jasperse, J.R., Robinson, R.M., Vondrak, R.R., Evans, D.S., 1987. Linear transport theory of auroral proton precipitation: A comparison with observations. J. Geophys. Res. 92, 5920–5932.

Bouhram, M., Berthelier, J.J., Illiano, J.M., Smith, H.T., Sittler, E.C., Crary, F.J., Young, D.T., 2005. The Enceladus satellite as a source of $N^+$ ions in Saturn's magnetosphere. Compt. Rend. Phys. 6, 1176–1181.

Burger, M.H., Sittler, E.C., Johnson, R.E., Smith, H.T., Tucker, O.J., 2006. Understanding the escape of water from Enceladus. J. Geophys. Res., in press.

Cosby, P.C., 1993. Electron-impact dissociation of nitrogen. J. Chem. Phys. 98 (12), 9544–9553.

Delitsky, M.L., Lane, A.L., 2002. Saturn's inner satellites: Ice chemistry and magnetospheric effects. J. Geophys. Res. 107 (E11), doi:10.1029/2002JE001855. 5093.

Dressler, R.A., Arnold, S.T., Murad, E., 1993. Guided-ion beam measurements of the $X(+) + H_2O(D_2O)$ (X = Ar, $N_2$) collision systems. J. Chem. Phys. 99, 1159–1171.

Dressler, R.A., Arnold, S.T., Murad, E., 1995. Charge-transfer dynamics in ion–polyatomic molecule collisions: $X + H_2O$ (X = N, Kr) luminescence study. J. Chem. Phys. 103 (23), 9989–10000.

Flesch, G.D., Ng, C.Y., 1990. A study of the reaction $O + (4S) + N_2$ using the tandem photoionization mass spectrometric method. J. Chem. Phys. 92, 3235–3236.

Freund, R.S., Wetzel, R.C., Shul, R.J., 1990. Measurement of electron-impact-ionization cross sections of $N_2$, Co, $CO_2$, CS, $S_2$, $CS_2$ and metastable $N_2$. Phys. Rev. 41 (11), 5861–5868.

Hansen, C.J., Esposito, L., Stewart, A.I.F., Colwell, J., Hendrix, A., Pryor, W., Shemansky, D., West, R., 2006. Enceladus' water vapor plume. Science 311 (5766), 1422–1425.

Ip, W., 1997. On neutral cloud distributions in the saturnian magnetosphere. Icarus 97, 42–47.

Johnson, R.E., Liu, M., Sittler Jr., E.C., 2005. Plasma-induced clearing and redistribution of material embedded in planetary magnetospheres. Geophys. Res. Lett. 32, doi:10.1029/2005GL024275. L24201.

Johnson, R.E., Smith, H.T., Tucker, O.J., Liu, M., Burger, M.H., Sittler Jr., E.C., Tucker, R.L., 2006. The Enceladus and OH tori at Saturn. Astrophys. J. 644, L137–L139.

Jurac, S., Richardson, J.D., 2005. A self-consistent model of plasma and neutrals at Saturn: Neutral cloud morphology. J. Geophys. Res. 110 (A9), doi:10.1029/2004JA010635. A09220.

Jurac, S., Johnson, R.E., Richardson, J.D., Paranicas, C., 2002. Satellite sputtering in Saturn's magnetosphere. Planet. Space Sci. 49, 319–326.

Matson, D.L., Castillo, J.C., Lunine, J., Johnson, T.V., 2006. Enceladus' plume: Compositional evidence for a hot interior. Icarus, in press.

Michael, M., Johnson, R.E., Leblanc, F., Liu, M., Luhmann, J.G., Shematovich, V.I., 2005. Ejection of nitrogen from Titan's atmosphere by magnetospheric ions and pick-up ions. Icarus 175 (1), 263–267.

Phelps, A.V., 1991. Cross sections and swarm coefficients for nitrogen ions and neutrals in $N_2$ and argon ions and neutrals in Ar for energies from 0.1 eV to 10 eV. J. Phys. Chem. Ref. Data 20, 557–573.

Porco, C.C., and 24 colleagues, 2006. Cassini observes the active south pole of Enceladus. Science 311 (5766), 1393–1401.

Rees, M.H., 1989. Physics and Chemistry of the Upper Atmosphere. Cambridge Univ. Press, New York.

Richardson, J.D., Sittler Jr., E.C., 1990. A plasma density model for Saturn based on Voyager observations. J. Geophys. Res. 95, 12019–12031.

Sheehan, C.H., St.-Maurice, J.-P., 2004. Dissociative recombination of $N^{2+}$, $O^{2+}$, and $NO^{+}$: Rate coefficients for ground state and vibrationally excited ions. J. Geophys. Res. 109 (A3), doi:10.1029/2003JA010132. A03302.

Shemansky, D.E., Matherson, P., Hall, D.T., Hu, H.-Y, Tripp, T.M., 1993. Detection of the hydroxyl radical in the Saturn magnetosphere. Nature 363, 329–332.

Shematovich, V.I., Johnson, R.E., Micheal, M., Luhmann, J.G., 2003. Nitrogen loss from Titan. J. Geophys. Res. 108 (E8), doi:10.1029/2003JE002094. 5087.

Sittler Jr., E.C., and 14 colleagues, 2005. Preliminary results on Saturn's inner plasmasphere as observed by Cassini: Comparison with Voyager. Geophys. Res. Lett. 32 (14), doi:10.1029/2005GL022653. L14S07.

Sittler Jr., E.C., and 11 colleagues, 2006a. Energetic nitrogen ions within the inner magnetosphere of Saturn. J. Geophys. Res. 111, doi:10.1029/2004JA010509. A09223.

Sittler Jr., E.C., and 15 colleagues, 2006b. Initial results on Saturn's inner plasmasphere as observed by Cassini: Comparison with Voyager. Planet. Space Sci. 54 (12), 1197–1210.

Smith, H.T., 2006. The search for nitrogen in Saturn's magnetosphere. Ph.D. thesis, University of Virginia, Charlottesville, VA.

Smith, H.T., Johnson, R.E., Shematovich, V.I., 2004. Titan's atomic and molecular nitrogen tori. Geophys. Res. Lett. 31 (16), doi:10.1029/2004GL020580. L16804.

Smith, H.T., Shappirio, M., Sittler, E.C., Reisenfeld, D., Johnson, R.E., Baragiola, R.A., Crary, F.J., McComas, D.J., Young, D.T., 2005. Discovery of nitrogen in Saturn's inner magnetosphere. Geophys. Res. Lett. 32 (14), doi:10.1029/2005GL022654. L14S03.

Spencer, J.R., Pearl, J.C., Segura, M., Flasar, F.M., Mamoutkine, A., Romani, P., Buratti, B.J., Hendrix, A.R., Spilker, L.J., Lopes, R.M., 2006. Cassini encounters Enceladus: Background and the discovery of a south polar hot spot. Science 311 (5766), 1401–1405.

Squyres, S., Reynolds, R., Cassen, P., 1983. The evolution of Enceladus. Icarus 53, 319–331.

Stevenson, D.J., 1982. Volcanism and igneous processes in small icy satellites. Nature 298, 142–144.

Stier, P.M., Barnett, C.F., 1956. Charge exchange cross sections of hydrogen ions in gases. Phys. Rev. 103 (4), 896–907.

Waite, J.H., and 13 colleagues, 2006. Cassini ion and neutral mass spectrometer: Enceladus plume composition and structure. Science 311 (5766), 1419–1422.

Young, D.T., and 57 colleagues, 2004. Cassini plasma spectrometer investigation. Space Sci. Rev. 114, 1–112.

Young, D.T., and 41 colleagues, 2005. Composition and dynamics of plasma in Saturn's magnetosphere. Science 307, 1262–1264.